Multiscale model intercomparisons of CO2 and H2O exchange in a maturing southeastern U.S. pine forest

Authors: Mario B. S. Siqueira, Gabriel G. Katul, D. A. Sampson, Paul C. Stoy, Jehn-Yih Juang, Heather R. McCarthy, and Ram Oren

Siqueira Mario B. S., Gabriel G. Katul, D. A. Sampson, Paul C. Stoy, Jehn-Yih Juang, Heather R. McCarthy, and Ram Oren (2006) Multi-scale model inter-comparisons of CO2 and H2O exchange in a maturing southeastern U.S. pine forest. Global Change Biology 12: 1189-1207. DOI: 10.1111/j.1365-2486.2006.01158.x.

Multiscale model intercomparisons of CO_2 and H_2O exchange rates in a maturing southeastern US pine forest

M. B. SIQUEIRA†, G. G. KATUL†, D. A. SAMPSON‡, P. C. STOY†, J.-Y. JUANG†, H. R. MCCARTHY† and R. OREN†

†*Nicholas School of the Environment and Earth Sciences, Duke University, Durham, NC 27708-0328, USA,*
‡*Virginia Tech, Department of Forestry, 319 Cheatan Hall, Blacksburg, VA 24061, USA*

Abstract

We compared four existing process-based stand-level models of varying complexity (physiological principles in predicting growth, photosynthesis and evapotranspiration, biogeochemical cycles, and stand to ecosystem carbon and evapotranspiration simulator) and a new nested model with 4 years of eddy-covariance-measured water vapor (*LE*) and CO_2 (*Fc*) fluxes at a maturing loblolly pine forest. The nested model resolves the 'fast' CO_2 and H_2O exchange processes using canopy turbulence theories and radiative transfer principles whereas slowly evolving processes were resolved using standard carbon allocation methods modified to improve leaf phenology. This model captured most of the intraannual variations in leaf area index (*LAI*), net ecosystem exchange (*NEE*), and *LE* for this stand in which maximum *LAI* was not at a steady state. The model comparisons suggest strong linkages between carbon production and LAI variability, especially at seasonal time scales. This linkage necessitates the use of multilayer models to reproduce the seasonal dynamics of *LAI*, *NEE*, and *LE*. However, our findings suggest that increasing model complexity, often justified for resolving faster processes, does not necessarily translate into improved predictive skills at all time scales. Additionally, none of the models tested here adequately captured drought effects on water and CO_2 fluxes. Furthermore, the good performance of some models in capturing flux variability on interannual time scales appears to stem from erroneous LAI dynamics and from sensitivity to droughts that injects unrealistic flux variability at longer time scales.

Introduction

Models that estimate the exchange of CO_2 between the atmosphere and terrestrial ecosystems are needed for developing relationships between anthropogenic CO_2 emissions and atmospheric CO_2 – a relationship required by policy makers to stabilize future atmospheric CO_2 (IPCC, 2001). At a more fundamental level, net ecosystem exchange of CO_2 (*NEE*) models represent the current state of understanding of ecosystem processes, and remain a central tool for predicting the response of ecosystems to disturbances and changing environments (Hanson *et al*., 2004). For these reasons, modeling *NEE* is currently a central topic in ecology, hydrology, and climate change research.

Key processes that are relevant to carbon transfer and storage in forested ecosystems can vary over multiple spatial and temporal scales. Upscaling these processes to estimate stand level *NEE* using process-based models is thus complex (Jarvis, 1995). Across time scales, NEE is influenced by fast processes such as turbulent transport mechanics (often measured in seconds) and slow processes such as forest growth (often measured in years to decades). In space, photosynthesis varies at the leaf scale (often measured in millimeters) whereas stand level variables such as tree density often vary over hundreds of meters (Baldocchi *et al*., 2000; Katul *et al*., 2001). This wide scale separation in time and space is complemented with a broad range of process-based models that have emerged to simulate different aspects of ecosystem carbon function. At the 'fast' end, some multilayer models, such as the CANVEG model

(Baldocchi, 1992; Baldocchi & Meyers, 1998), consider within-canopy physiological and radiative transfer processes starting from leaf-level equations and integrate these processes up to the stand level using turbulent dispersion theories. These models provide vertically explicit carbon and water flux estimates (as well as concentrations) within and above the canopy over the course of the day and they resolve all nonlinear interactions between intracanopy radiative transfer processes, photosynthesis-light response, skin temperature and energy balance, and drag and attenuation of flow statistics. At the 'slow' end, zero-dimensional forest growth models such as physiological principles in predicting growth (3-PG) (Landsberg & Waring, 1997) utilize a species-specific potential carbon uptake rate without resource limitations, then modify this rate by a set of reduction functions imposed by climatic, hydrologic, and resource constrains. Here, zero-dimensional models are models that do not include any spatial structure; they represent the biosphere by a big leaf or reservoir of known capacity or size. Multilayer models are one-dimensional models that do resolve the vertical structure of the canopy, often via the leaf area density. Analogous to the spatial representation, the 3-PG model uses a coarse integration time step (i.e. monthly) to compute individual components of *NEE*. Although this time scale is too coarse for resolving diurnal cycles of light, temperature, vapor pressure deficit (*D*), or wetting fronts in soils, it may be sufficient to assess the long-term impact of forest management on forest production (Landsberg *et al*., 2001).

Comparing models with different assumptions and simplifications in their formulation contributes to understanding the controls over ecosystem productivity and helps identify critical gaps in our knowledge. Model comparison is also timely for two data-related reasons: (1) Many FluxNet (a global network of eddy-covariance (EC) flux measurements) tower sites across a wide range of biomes have gathered long term (e.g. more than 4 years) of *NEE* data and associated climatic and ecological measurements; and (2) satellite remote sensing is now providing global coverage of ecological variables at a spatial resolution comparable to the footprint of EC flux measurements of *NEE*. Models are the primary tools for merging information from these data sets into terrestrial carbon exchange, and comparing model performances is important for assessing our ability to estimate ecosystem productivity.

A recent study compared the output of 13 models against a 10-year data record that included *NEE* estimated over a hardwood forest in the southern US, assumed to be in equilibrium, (i.e. leaf area no longer changed with age but mainly with climatic, hydrologic, and other disturbances (Hanson *et al*., 2004)). The study concluded that models that resolve the light/canopy structure performed better at short time scales than the standard coarse-grained (or zero-dimensional) models. However, their findings at longer time scales were surprisingly mixed, suggesting that the next step in model intercomparisons must establish a framework to: (1) methodically investigate 'across-scale' information flow for various models, and (2) use such information to construct hybrid models that can utilize 'skills' from various model components at appropriate time scales. Addressing the first point will advance understanding on how 'subgrid filtering,' which refers to the effect of the unresolved fine scale (in time and space) processes to model outputs, affects model performance at resolved scales. Addressing the second point invites the potential use of formal 'nesting' schemes to link fast processes (e.g. diurnal variation of photosynthesis) to the slowly evolving ones (e.g. carbon allocation). The nesting approach should be useful because of the wide scale separation between variability at diurnal scales (important for radiative transfer) and monthly scales (important for carbon allocation).

We investigated the performance of a broad array of process-based models to assess their prognostic ability to reproduce variability in biosphere–atmosphere exchange of carbon and water for a maturing loblolly pine plantation that has a subcanopy hardwood component in the Southern Piedmont region of North Carolina. We employed a spectral comparison because it enables identifying the time scales at which the model can reproduce measured flux variability correctly. Often, models with several parameters can be calibrated to reproduce the mean flux values at the desired scale (e.g. hourly or annual). However, model-generated relationships between internal variables (e.g. *LAI*), external forcing, and flux variability may not be sensitive to such calibration at other time scales (e.g. at seasonal or interannual time scales). We considered four existing models that vary in complexity, number of parameters, and spatio-temporal integration of the canopy processes. Formally, algorithmic complexity is connected with the number of rules needed to define the state dynamics in a model. These four models are:

(1) 3-PG (Landsberg & Waring, 1997),
(2) Photosynthesis and Evapotranspiration (PnET II; Aber & Federer, 1992),
(3) Biogeochemical cycles (Biome-BGC; Running & Coughlan, 1988), and
(4) Stand to Ecosystem Carbon and Evapotranspiration Simulator (SECRETS-3PG; Sampson *et al*., 2001).

In addition to the above models, we developed a nested model, hereafter referred to as CANVEG-A (CANVEG with carbon allocation). To resolve fast processes the

model uses CANVEG, which is a coupled ecophysiological, biogeochemical, and atmospheric diffusion model (Baldocchi, 1992), later revised for realistic physiology (Baldocchi & Meyers, 1998) and to include detailed second-order closure principles (Lai *et al*., 2000). To resolve the slow processes we nested CANVEG within a simple allocation scheme similar to 3-PG. These five forest ecosystem models were chosen because they populate almost the entire domain of model complexity given their process algorithms and their space–time resolution (see Table 1).

Currently, Biome-BGC and PnET II are used to scale-up carbon uptake on continental scales using remotely sensed *LAI* measurements (e.g. from MODIS). It is not our intent here to assess how well these models reproduce *NEE* when forced by *LAI* measurements because *LAI* must be one of the predicted variables when assessing how forested ecosystems respond to future disturbances or changing environments.

We used a pine plantation as a case study because, in addition to their economic importance, they represent a 'simple' system (in terms of dominant species) for which ample data are available. A 4-year EC data set (from 2000 to 2003) collected at the Duke Forest pine site along with ecological measurements was used in this model comparison. On the basis of the annual precipitation measurements, the selected 4 years include a mild drought at the beginning of the growing season (2001), a severe drought (2002, the fifth most severe drought on record), and two wet years (2000 and 2003). Hence, a wide range of climatic and hydrologic conditions was sampled within the study period.

Methods

Experimental Site

The study site is located at the Blackwood division of Duke Forest near Durham, North Carolina, USA (35°58′N, 79°05′W, elevation = 163 m above sea level) and is part of the *AmeriFlux* network (Baldocchi *et al*., 2001). The site was uniformly planted with loblolly pine (*Pinus taeda* L.) in 1982; the current density is ~ 1733 trees ha^{-1}. In addition to the dominant pine species, an understory hardwood canopy of 26 different species has developed. The stand is located on Enon silt loam, a low fertility Hapludalf with 11.2% clay, 45.8% silt, and 43.0% sand (Hacke *et al*., 2000), with a depth of approximately 0.7 m where the bedrock typically resides (Oren *et al*., 1998). The long-term annual precipitation averages 1140 mm and is evenly distributed throughout the year (Oren *et al*., 1998). The rooting zone is limited by a clay pan at 0.3 m, which reduces soil hydraulic conductivity by an order of magnitude and

Table 1 Characteristics and key process parameterizations of the models

Models	3-PG	PnET II	Biome-BGC	SECRETS-3PG	CANVEG-A
Characteristics					
Time step/scale resolved	Month/year	Month/month	Day/week	Hour/day	Hour/day
Number of compartments	3	5	28	5	4
Vertical discretization	Single layer	Single layer	Single layer	Two-layer	Multi-layer
Process parameterizations					
Photosynthesis	Light use efficiency	Foliar N concentration	Biogeochemistry	Biogeochemistry	Biogeochemistry
Maintenance respiration	Fraction of GPP	Fraction of GPP, Q_{10}	Function of N content, Q_{10}	Q_{10}	Q_{10}
Growth respiration	–	Fraction of Allocation	Fraction of Allocation	Fraction of Allocation	Fraction of Allocation
Allocation	Allometry	*GDD*	Allocation parameters	Allometry	*GDD*, allometry
Litterfall	Fraction of leaf standing biomass	Foliage retention time	Fraction of leaf standing biomass	Leaf cohorts	Fraction of reference leaf biomass
Water balance	Penman–Monteith	Water use efficiency	Penman–Monteith	Conductance model	Conductance model

Acronyms are described in the text. GDD is growing degree days.

strongly couples transpiration and stomatal conductance to recent precipitation (Oren *et al*., 1998). The local climate is characterized by warm, humid summers with relatively moderate winters (Ellsworth *et al*., 1995). The topographic variations are small (terrain slope changes $<5\%$) so that the influence of topography on micrometeorological flux measurements can be neglected (Kaimal & Finnigan, 1994). Measurements were performed on a 23.3 m walkup tower in an ambient CO_2 plot (plot 1) at the edge of the free Air CO_2 enrichment (FACE) study at Duke Forest; the plot is not affected by the CO_2 enrichment in treated plots.

Micrometeorological, radiative, and hydrological measurements

Air temperature (T_a) and relative humidity (HP45C, Vaisala, Helsinki, Finland) were measured at 2/3 canopy height and were used to compute *D*. A photosynthetic photon flux density sensor (Q190, Li-Cor, Lincoln, NE, USA) to measure photosynthetically active radiation (PAR), a net radiometer (REBS Q7, Radiation and Energy Balance System, Seattle, WA, USA), and a total radiation sensor (CNR1, Kipp & Zonen, Delft, the Netherlands) for radiation/energy budget calculations were located at the top of the tower, about 6.0 m above the mean canopy height (in 2001). These sensors sampled at 1 Hz and the outputs were averaged every half hour. Precipitation was measured with a tipping bucket (TI, Texas Electronics, Dallas, TX, USA), summed half-hourly, and corrected or gap-filled with daily measurements from a nearby graduated rain gauge to assure consistent daily rainfall for all models. The data from the tipping bucket gauge require occasional adjustments because: (1) missing data inject a negative bias (i.e. precipitation is reduced); (2) the small volume of the tipping scale may be further reduced by insects or dirt, thus tipping at a lower rainfall intensity and injecting a positive bias; and (3) the intercepting surface of the gauge may occasionally collect uplifted leaves, intercepting a portion of precipitated water and injecting a negative bias. The latter two factors are stochastic and periodic cleaning is insufficient to address the errors they cause.

Turbulent flux measurements

The momentum, CO_2 (*Fc*), latent (*LE*) and sensible (*H*) heat fluxes were measured by a standard EC system comprised of a CO_2/H_2O infrared gas analyzer and a triaxial sonic anemometer (CSAT3, Campbell Scientific, Logan, UT, USA). A closed path gas analyzer (Licor-6262, Li-Cor) and a krypton hygrometer (KH2O, Campbell Scientific) were employed before May 1, 2001. The latter was used to assess and correct tube attenuation effects and lagged maximum cross-correlation between vertical velocity and the measured scalar concentration. Raw 5-Hz measurements were postprocessed using procedures described elsewhere (Katul *et al*., 1997). The system was positioned at 15.5 m, about 1 m above the canopy at that time. For subsequent years, an open path gas analyzer (Licor-7500, Li-Cor) was employed, and the system was shifted upward to 20.2 m to accommodate forest growth. With this configuration, a 10 Hz sampling rate was used and real-time processing of the fluxes and flow statistics was performed (CR23X, Campbell Scientific). The Webb–Pearman–Leuning (Webb *et al*., 1980) postprocessing correction was applied to *Fc* and *LE* to account for the density variation effects on EC flux measurements. A footprint analysis (Hsieh *et al*., 2000) showed that, under near neutral atmospheric stability conditions, the peak of the source-weight function (i.e. the maximum flux source area) rarely exceeded 120 m.

Ecophysiogical measurements

Temporal dynamics of leaf area index (*LAI*) were generated using leaf litterfall mass and specific leaf area, needle elongation rates, fascicle, flush and branch counts, allometry, and optical gap fraction measurements (H. McCarthy, personal communication). Allometric relations (Naidu *et al*., 1998) were used to estimate net primary production (*NPP*). Biomass estimates and above- and belowground respiration rates, described elsewhere (Ryan *et al*., 1996; Hamilton *et al*., 2001, 2002), were used to quantify respiration. The maximum rate of ribulose-1,5-bisphosphate-carboxylase-oxygenase (Rubisco) activity ($V_{c,max}$) was available from leaf-level gas-exchange measurements (Ellsworth, 2000).

NPP measured by biometry methods is also reported. This value corresponds to the average of three ambient rings at the Blackwood division of the Duke Forest. We found it more appropriate to report the average of the three rings given that our footprint analysis suggests that during daytime conditions, over 50% of the scalar sources contributing to the EC measurements are beyond the boundaries of one ring.

Models

To investigate the predictive skills of the five process-based models at various time scales, we evaluated their ability to reproduce the measured spectral properties of *NEE* and *LE*. Unlike previous comparisons that assess how well models reproduce annual, monthly, or diurnal *NEE* (or *LE*), spectral analysis permits us to assess how well these models reproduce the variability (activity or energy) at all of the relevant time scales. This approach

can be used to assess both how well models reproduce the temporal autocorrelations in the *NEE* (or *LE*) time series and the degree of deviation from long-term averages over a wide range of time scales. We employed Fourier spectral comparison because we can interpret the squared Fourier coefficient (representing the spectral energy) for each frequency as the portion of the variance explained by that frequency. A review of spectral analysis in the geosciences can be found elsewhere (Stull, 1988). Thus, spectral analysis determines the time scales best reproduced by each model for each variable. Spectral analysis also permits us to assess whether resolving short-term dynamics with CANVEG-A improves long-term flux predictions. For this purpose, we used Fourier transformation averaged to the relevant time scales for biosphere–atmosphere gas exchange to discern model performance in reproducing the EC measured spectral variability.

The assumptions and formulation of 3-PG, PnET II, Biome-BGC, and SECRETS-3PG are published elsewhere; however, a brief overview of the processes most relevant to the data-model comparisons is presented below. Following this summary, we describe the CANVEG-A, including its carbon allocation routine, which is based on 3-PG. Table 1 summarizes the salient features for each model.

3-PG(v2)

The 3-PG model (Landsberg & Waring, 1997) calculates the maximum gross primary production (*GPP*) from absorbed photosynthetically active radiation (*APAR*), and quantum efficiency (i.e. conversion efficiency of moles of *APAR* photons to moles of carbon assimilated by the plant). *APAR* depends upon incident radiation, *LAI*, and canopy light extinction. Actual *GPP* is obtained by applying environmentally controlled reductions to include the effects of soil drought, *D*, T_a, soil nutrition, and stand age. The environmental reduction functions proportionally reduce maximum potential *GPP* as conditions depart from optimum on a scale from zero to one. The modifier functions use the climatic inputs and forest physiological responses to those inputs using first principles. Because the model was developed to predict stand development for forestry applications, some eco-physiological parameters that are expected to change as the forest ages are allowed to vary through time.

3-PG assumes a constant ratio between *GPP* and *NPP* for calculating the actual organic mass incorporated by the plants. This assumption may be reasonable at the annual time scale (Waring *et al*., 1998), even though arguments supporting the constant *NPP*/*GPP* are often artificially constrained (Medlyn & Dewar, 1999). The carbon allocation to foliage, stem, and roots is based on allometric relationships that vary among species. The model considers litterfall and root turnover as a fraction of leaf and root biomass, respectively.

The soil water balance, used to adjust the soil drought modifier, is obtained as the difference between monthly transpiration calculated using the Penman–Monteith equation (Campbell & Norman, 1998) and monthly precipitation. A simple bucket model is used to estimate available soil water for plants based on soil depth and soil texture. Monthly outputs are integrated to annual estimates of stand performance.

PnET II (v5.0–1.5vb)

PnET II (Aber & Federer, 1992; Aber *et al*., 1995) is a monthly time-step model that assumes that water and carbon balances are primarily driven by nitrogen availability (expressed as foliar nitrogen concentration). It applies the generalized linear relationship between foliar nitrogen content and maximum net photosynthesis (Field & Mooney, 1996). The coefficients of the linear equation are species specific and the foliar nitrogen concentration is user specified.

Maintenance respiration of leaves, used to estimate actual net carbon assimilation, is calculated as a fraction of maximum net photosynthesis. The respiration is further corrected for temperature by a Q_{10} factor. The maximum photosynthesis is then modified for suboptimal environmental conditions using reduction functions similar to 3-PG. The environmental variables considered in the reduction functions are T_a, water availability, and *D*.

LAI and light restriction are incorporated through a light attenuation model (Campbell & Norman, 1998). Although photosynthesis and leaf respiration are computed at sequential canopy layers and integrated to the whole canopy, the model does not consider the actual vertical structure of the foliage distribution. For this reason, we considered PnET II as single-layer model for the purpose of this model intercomparison. The model is used to determine the amount of carbon actually assimilated along with the potential gross photosynthesis (gross photosynthesis without water restrictions) used in the water balance calculations.

Carbon allocation to foliar and wood biomass is driven by the accumulation of growing degree-days (the sum of daily mean T_a above 0 °C, beginning January 1st each year). The user specifies growing degree-day sums at which foliar production begins and ends. The carbon produced and held in reserve throughout the year is then allocated to leaves as a linear function of the accumulated growing degree-days between the predetermined sums. This procedure is repeated for wood production.

Allocation to roots is estimated as a linear function of foliar production with user-specified parameters. Litterfall is considered a function of foliage retention time.

The water balance is obtained by calculating interception, drainage, and throughfall as fractions of precipitation. Transpiration is estimated from water use efficiency and potential gross photosynthesis (i.e. water use is function of assimilated carbon). Soil water is estimated using a simple bucket model for soil water, limited by water holding capacity estimated from soil characteristics. A limit to the transpiration is further employed to express the maximum transpiration as a fraction of available water.

Biome-BGC (v4.1.1)

Biome-BGC is a fully coupled carbon-water-nitrogen cycle model (Running & Coughlan, 1988; Kimball *et al*., 1997a,b; Thornton *et al*., 2002). The model considers canopy interception and evaporation, transpiration, photosynthesis, growth and maintenance respiration, carbon allocation above- and belowground, decomposition and nitrogen mineralization mechanistically, incorporating minimal species-specific data.

Biome-BGC uses biogeochemical principles to estimate leaf level photosynthesis based on limiting factors such as light availability and nitrogen restrictions to enzyme activity. Mass diffusion through stomata is explicitly considered at the leaf level – although the model itself does not have a vertical structure. To scale up from leaf to canopy level assimilation, the model separates leaf area into shaded and sunlit foliage, providing a more realistic representation of canopy structure albeit via a big-leaf representation. Carbon allocation is then computed through complex interactions between the multiple carbon pools via transfer mechanisms and limitations imposed by nutrients. Decomposition is also a function of nitrogen content of the various dead organic matter pools with values determined from the nitrogen cycle routine.

Canopy evapotranspiration (*ET*) is calculated using a Penman–Monteith model (as in 3-PG). As in 3-PG and PnET II, soil water is calculated, using a bucket model with soil properties derived from soil texture and composition. Environmental reductions because of soil drought, *D*, and T_a are applied to stomatal conductance, which is then used for both carbon and water mass transfer equations. The entire set of equations is integrated on a daily time step.

SECRETS-3PG

The SECRETS-3PG is a hybrid model that combines the process model SECRETS (Sampson & Ceulemans, 1999; Sampson *et al*., 2001, 2006) and elements from the 3-PG forest growth model (Landsberg & Waring, 1997). As a multispecies, multiple-structure process model, SECRETS simulates stand-scale carbon and water fluxes using process algorithms adapted from several sources: Farquhar photosynthesis with sun/shade partitioning; (dePury & Farquhar, 1997), water balance (Meiresonne *et al*., 2003) and maintenance respiration formulations from the BIOMASS model (McMurtrie & Landsberg, 1992), and either empirical or mechanistic soil respiration (Thornley, 1998). Here we used a five-parameter (Sit & Poulin-Costello, 1994) empirical model for soil respiration (R_S):

$$R_S = \beta_0(T_{SOIL}^{\beta 1}\beta_2^{T_{SOIL}})(\theta^{\beta 3}\beta_4^{Vol}), \quad (1)$$

where T_{SOIL} is soil temperature at 10 cm, θ is volumetric soil water content estimated at 17 cm, and β_0–β_4 were parameters to be estimated. The parameters were optimized using half-hourly soil respiration measurements made with an Automated CO_2 exchange system or ACES (Butnor *et al*., 2003) at the Duke FACE experiment during 2001 and 2002 (Palmroth *et al*., 2005) with a resulting $r^2 = 0.75$ for the regression fit. The SECRETS model simulates photosynthesis every hour, but computes maintenance respiration, water balance, and soil respiration daily.

The SECRETS-3PG hybrid model was designed to be a forest management tool while maintaining basic leaf-level physiology. Thus, SECRETS-3PG links the process-level functions from SECRETS and carbon allocation algorithms (and associated functions) from 3-PG. However, unlike 3-PG, SECRETS-3PG partitions carbon into foliage, stems, branches, fine roots, coarse and tap roots, and bark. The model structure enables: (1) rotation-length silvicultural prescriptions (i.e. planting, harvesting, thinning, and fertilization amendments), (2) biometric estimates of stand structure (i.e. volume growth, quadratic mean diameter, dominant height, etc.), and ecosystem fluxes of CO_2 and H_2O. Thus, it enables model-data comparisons of stand structure attributes and process-level mechanisms using field measurements at scales appropriate to both. As a modification from the standard 3-PG model, SECRETS-3PG incorporates a dynamic needle litterfall that is representative of a three foliage cohort to improve pine leaf dynamics (Sampson *et al*., 2003).

Simultaneous simulations for over- and understory species are possible using SECRETS-3PG. For these simulations, we used the pine carbon allocation scheme for the pine simulations but used estimates of *LAI* from litterfall collected at the site for the hardwood simulations. Because no allocation is currently possible for subcanopy species, the understory allocation was simplified by assuming that its *NPP* represents 47% of *GPP* (Landsberg & Waring, 1997).

Water balance, important for the soil respiration estimates, represents hardwood and pine water use, as well as soil water lost to evaporation from boles and wet canopies (during rain events), and from the surface of the litter. The sequential simulations necessitate a hierarchy of access to available soil water. SECRETS-3PG assumes that subcanopy species (hardwoods) have first access to the soil water. Because the present version of SECRETS-3PG does not account for soil moisture effects on assimilation, this 'water access hierarchy' does not impact carbon cycling unless soil moisture nears the permanent wilting point. This condition was rare during the study period.

CANVEG with carbon allocation (CANVEG-A)

We used a formulation that couples conservation equations for heat and mean scalars (CO_2 and water vapor), leaf energy and radiation budgets, with biophysical and physiological mechanisms responsible for carbon assimilation (i.e. the Farquhar model) nested within a carbon allocation routine that distributes carbon into four different pools.

To resolve the effect of turbulent transport processes (i.e. representing the effects of turbulent eddies with a time scale of seconds on 30 min averaging time scales), CANVEG uses second-order closure principles (Katul & Chang, 1999; Katul & Albertson, 1999; Siqueira & Katul, 2002) integrated to half-hourly time steps. Models that use second-order closure principles solve for the mean wind speed and all six components of the turbulent Reynolds stresses needed for linking vertical scalar source (or sink) distribution to mean concentration (e.g. water vapor and atmospheric CO_2) or temperature inside canopies. Conversely, the carbon allocation was set to vary on a monthly time step. This time step was deemed sufficiently short to resolve foliage growth, the most dynamic of the four carbon pools (Stoy *et al*., 2005).

In the current implementation of CANVEG, we used a light model (Stenberg, 1998) that resolves penumbral effects, a Eulerian closure model for scalar transfer including local thermal stratification inside the canopy, and a more physiologically sound Leuning conductance model (Leuning, 1995; Oren *et al*., 1999; Katul *et al*., 2000; Stoy *et al*., 2005) in lieu of the original Ball-Berry model (Collatz *et al*., 1991). Hence, CANVEG does not assume 'well-mixed conditions' inside the canopies and actually solves for the vertical distribution of mean temperature, CO_2, and H_2O concentration profiles (unlike the remaining four models). Because CANVEG resolves the vertical structure of the scalar sources within the canopy we were able to separate the forest into overstory pine and an understory hardwood within the nested scheme. This multispecies approach enabled us to account for differences in both seasonal dynamics and physiology of these two distinct vegetation components. Maintenance respiration rates of different tissues of both pines and hardwoods, needed in *NPP* estimations, were computed as functions of temperature using the Q_{10} formulation. Foliage temperature was calculated as part of the energy budget, root temperature was assumed to be at soil temperature and stem/branch temperature was a weighted average of air (with a delay) and soil temperatures to account for wood heat capacity and sap flow cooling.

CANVEG-A explicitly considers four carbon pools for each vegetation component: foliage, stem, roots, and a labile pool. Similar to 3-PG, belowground allocation assumes that the more nutrient limited the soil environment, the greater the fraction of *NPP* allocated to the root system (Landsberg & Waring, 1997). As in 3-PG, environmental condition modifiers are defined as functions of air humidity deficit, site fertility and stand age, given by

$$f_{\mathrm{D}} = \mathrm{e}^{-kD}, \tag{2}$$

$$m = m_0 + (1 - m_0)FR, \tag{3}$$

$$f_{\mathrm{age}} = \left[1 + \left(\frac{A}{A_{\max} r_A}\right)^{n_A}\right]^{-1}, \tag{4}$$

where f_{D}, m, and f_{age} are humidity deficit, fertility and age modifiers respectively, *FR* is a site fertility rating, A is stand age, $A_{\max}$ is the maximum age likely to be attained by the stand, and k, m_0, r_A, and n_A, are empirical coefficients related to the sensitivity of each species to these factors.

Even though these modifiers were primarily developed in 3-PG to constrain light use efficiency, they were also used for partitioning *NPP* between below- and aboveground components. Here, these modifiers are used as interpolation factors for the proportion of *NPP* allocated to roots (η_{r}) between user-defined minimum ($\eta_{\mathrm{r,min}}$) and maximum ($\eta_{\mathrm{r,max}}$) values:

$$\eta_{\mathrm{r}} = \frac{\eta_{\mathrm{r,max}}\eta_{\mathrm{r,min}}}{\eta_{\mathrm{r,min}} + (\eta_{\mathrm{r,max}} - \eta_{\mathrm{r,min}}) f_{\mathrm{D}} f_{\mathrm{age}} m}. \tag{5}$$

The rate of change of root biomass is then

$$\frac{\mathrm{d}W_{\mathrm{r}}}{\mathrm{d}t} = \max(\eta_{\mathrm{r}} NPP, 0) - \gamma_{\mathrm{r}} W_{\mathrm{r}}, \tag{6}$$

where W_{r} is root biomass (in carbon units) and η_{r} is monthly root turnover (assumed constant). Because of the relatively short monthly integration time step, the maximum function in Eqn (6) is necessary to prevent root biomass loss because of negative *NPP* during low leaf area periods.

The labile pool is a representation of the substrate reserve stored by the tree and receives second priority after the root system in terms of carbon allocation. To avoid negative values of this pool, its amount is kept at a level that will be enough to completely replace the foliage. The foliage carbon pool is divided into 'new' and 'old' leaf cohorts and the transition from 'new' to 'old' cohort occurs at a user specified month of the year. Litterfall is estimated as a proportion of the 'old' leaf cohort immediately after the time of the 'new to old' foliage transition. A look-up table for each vegetation type gives a monthly proportionality factor. Foliage production removes carbon from the labile pool to build a 'new' leaf cohort with the timing for foliage emergence determined by heat sums (growing degree days to start and end foliage production) analogous to PnET II. The actual amount of foliage produced is constrained by environmental conditions, for which the D modifier is used as a surrogate along with a species-specific sensitivity. The allometric relationship between foliage and stem mass as function of diameter at breast height (DBH) bounds the amount of foliage to be produced.

Equations (7)–(10) present the rate of change of leaf cohorts and substrate biomasses:

$$\frac{\mathrm{d}W_{\mathrm{f,new}}}{\mathrm{d}t} = f_{\mathrm{T}}\left(W_{\mathrm{f,max}} - W_{\mathrm{f,new}}\right)f_{\mathrm{D}}^{b}, \tag{7}$$

$$\frac{\mathrm{d}W_{\mathrm{f,old}}}{\mathrm{d}t} = -\gamma_{\mathrm{f}}W_{\mathrm{f,0}}, \tag{8}$$

$$W_{\mathrm{f,old}} = W_{\mathrm{f,new}},$$

$$W_{\mathrm{f,new}} = 0 \text{ at a user prescribed month of year}, \tag{9}$$

$$\frac{\mathrm{d}W_{\mathrm{l}}}{\mathrm{d}t} = \min\left(W_{\mathrm{f,max}} - W_{\mathrm{l}}, NPP - \frac{\mathrm{d}W_{\mathrm{r}}}{\mathrm{d}t}\left(1 + r_{\mathrm{s,r}}\right) - \frac{\mathrm{d}W_{\mathrm{f,new}}}{\mathrm{d}t}\left(1 + r_{\mathrm{s,f}}\right)\right) \tag{10}$$

where $W_{\mathrm{f,new}}$, $W_{\mathrm{f,old}}$ and W_{l} are 'new' leaf cohort, 'old' leaf cohort, and labile carbon biomasses, respectively $W_{\mathrm{f,max}}$ is the maximum amount of new leaf (a function of DBH), b is species-specific sensitivity to environmental conditions, $W_{\mathrm{f,0}}$ is the reference biomass for litterfall, and η_{f} is the proportionality factor of litterfall for each month. Note that the η_{f} look-up table values add up to unity; thus $W_{\mathrm{f,0}}$ is shed within the year and leaf biomass conservation is guaranteed. The $r_{\mathrm{s,r}}$ and $r_{\mathrm{s,f}}$ are construction costs associated with the synthesis of root and leaf tissues, respectively. Equation (10) ensures that carbon needed to cover carbon expenses in excess of *NPP* is derived from the reserve pool that is replenished as soon as *NPP* becomes positive. f_{T} is the timing function for foliage development and is given by

$$f_{\mathrm{T}} = \begin{cases} 0 & \text{if } GDD < GDD_{\mathrm{stt}} \text{ or } GDD > GDD_{\mathrm{end}}, \\ \frac{GDD - GDD_{\mathrm{stt}}}{GDD_{\mathrm{end}} - GDD_{\mathrm{stt}}} & \text{if } GDD_{\mathrm{stt}} < GDD < GDD_{\mathrm{end}}, \end{cases} \tag{11}$$

where GDD stands for growing degree days, and GDD_{stt} and GDD_{end} are growing degree days for start and end of leaf production. Foliage is distributed vertically according to a user-specified leaf area density (*LAD*) shape function for under- and overstory (assumed triangular in this study).

The remaining *NPP*, if any, is then allocated to stem and branches using

$$\frac{\mathrm{d}W_{\mathrm{s}}}{\mathrm{d}t} = \max\left(0, \frac{NPP - \frac{\mathrm{d}W_{r}}{\mathrm{d}t}\left(1 + r_{\mathrm{s,r}}\right) - \frac{\mathrm{d}W_{\mathrm{f,new}}}{\mathrm{d}t}\left(1 + r_{\mathrm{s,f}}\right) - \frac{\mathrm{d}W_{\mathrm{l}}}{\mathrm{d}t}}{\left(1 + r_{\mathrm{s,s}}\right)}\right), \tag{12}$$

where W_{s} is wood biomass and $r_{\mathrm{s,s}}$ is construction respiration for woody tissue.

CANVEG is used to solve for canopy photosynthesis, respiration, and *ET* every 30 min. The monthly integrated values are transferred to carbon allocation modules, which then predict foliage dynamics and forest growth. The resulting changes in the carbon pools in the form of *LAD* and respiring biomass are then remapped back into CANVEG. This approach takes maximum advantage of the scale separation between the slowly evolving growth and allocation processes and the rapid (and nonlinear) response of photosynthesis, *ET*, and respiration to diurnal variations in light, D, wind speed, and T_{a}. The choice of monthly time step for biomass pool updates allowed us to develop efficient algorithms for the model calculations that take advantage of optimized fast matrix operations. *LAI* is the most dynamic of the biomass pools. At this pine plantation, the monthly spectral energy of *LAI* is 10-fold that of the daily spectral energy and a tenth of the seasonal value (Stoy *et al*., 2005), making the monthly time step optimal in terms of maximizing computational efficiency while retaining the key modes of variability in the 'fast pools.'

This allocation scheme provides several desirable features for pine forests. First, the model ensures that a reserve pool provides the carbon needed to produce foliage; hence, leaf display dynamics is decoupled from production on short time scales. Also, litterfall is no longer synchronous with leaf standing biomass (as is the case in 3-PG). The effect of these two revisions is illustrated in Fig. 1, which shows the monthly time series of *LAI*, normalized *NPP*, and *ET* for 3-PG, CAN-

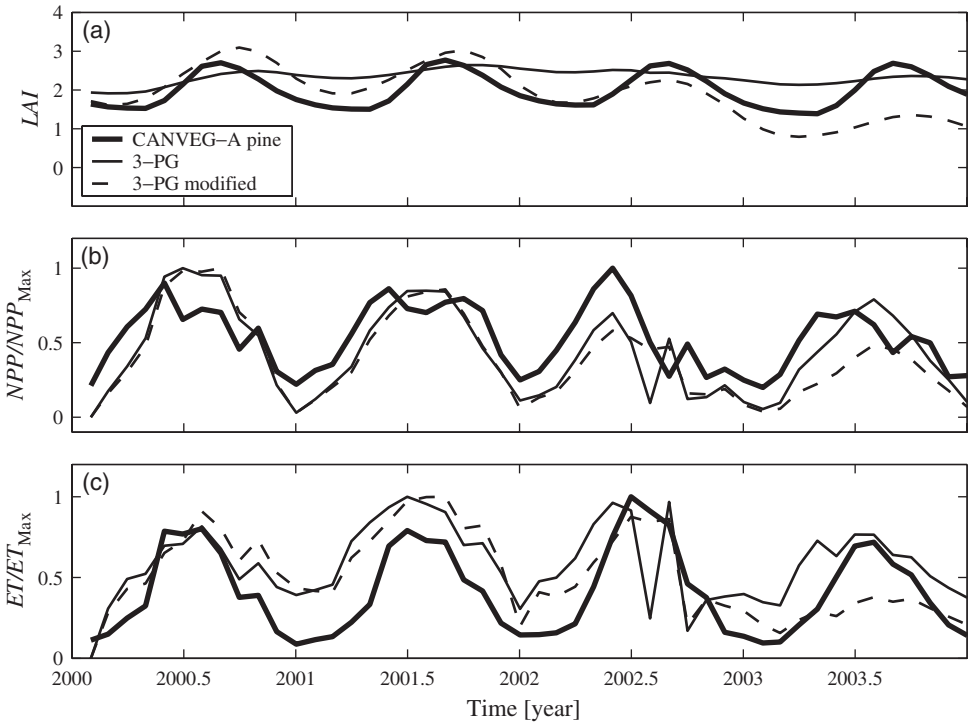

Fig. 1 Time series for pine leaf area index (*LAI*), normalized net primary production (*NPP*), and normalized evapotranspiration (*ET*) for the CANVEG with carbon allocation (CANVEG-A), the original physiological principles in predicting growth (3-PG), and 3-PG modified to include a new litterfall parameterization.

VEG-A, and the 3-PG model version modified to include the litterfall scheme developed for CANVEG-A. It is clear that the new litterfall formulation improved the description of the short-term leaf area dynamics when compared with the original version of 3-PG. However, because of the strong coupling between leaf production, *ET* and *NPP* in 3-PG, the recovery process from adverse conditions, such as the severe drought during the 2002 growing season, is unrealistically slow (Fig. 1). Note, for example, the low *LAI*, *NPP*, and *ET* values for the modified 3-PG model in year 2003 relative to their initial values. It is clear that modifying litterfall dynamics alone can possibly improve predictions on shorter time scales but may diminish the accuracy of predictions of forest development on longer time scales. On the other hand, the new allocation algorithm embedded in CANVEG-A retains the expected long-term coupling between standing foliage and its production. Additionally, the scheme is general enough to handle both evergreen and deciduous vegetation.

Results and discussion

We begin by assessing the performance of the CANVEG-A scheme, concentrating on *LAD*, *LAI*, and biosphere–atmosphere carbon and water exchange rates. Following this we present and discuss the results from the model intercomparisons. Parameters required to run the models were obtained from direct eco-physiological measurements (Ryan *et al*., 1996; Naidu *et al*., 1998; Ellsworth, 2000; Hamilton *et al*., 2001, 2002) or, when those were not available, from default values of each model.

CANVEG-A validation

CANVEG-A reproduced the measured *LAD* (for both pines and hardwoods) over the study period (Figs 2a and b). One notable exception was the model failure to reproduce the relatively large *LAI* of the hardwood understory in year 2001. Nevertheless, this underestimation in 2001 is not likely to have had a significant impact on carbon uptake (and production) because the understory assimilation is a small fraction of total canopy photosynthesis because little light penetrates the main canopy layer (Schäfer *et al*., 2003). However, we note that the light model employed in CANVEG neglects sun-flecks known to be important for understory photosynthesis (Naumburg *et al*., 2001).

CANVEG-A accurately reproduced the measured *Fc* and *LE* (Figs 3a and c, respectively) at times without water stress. Statistical measures (see Table 2, first set of

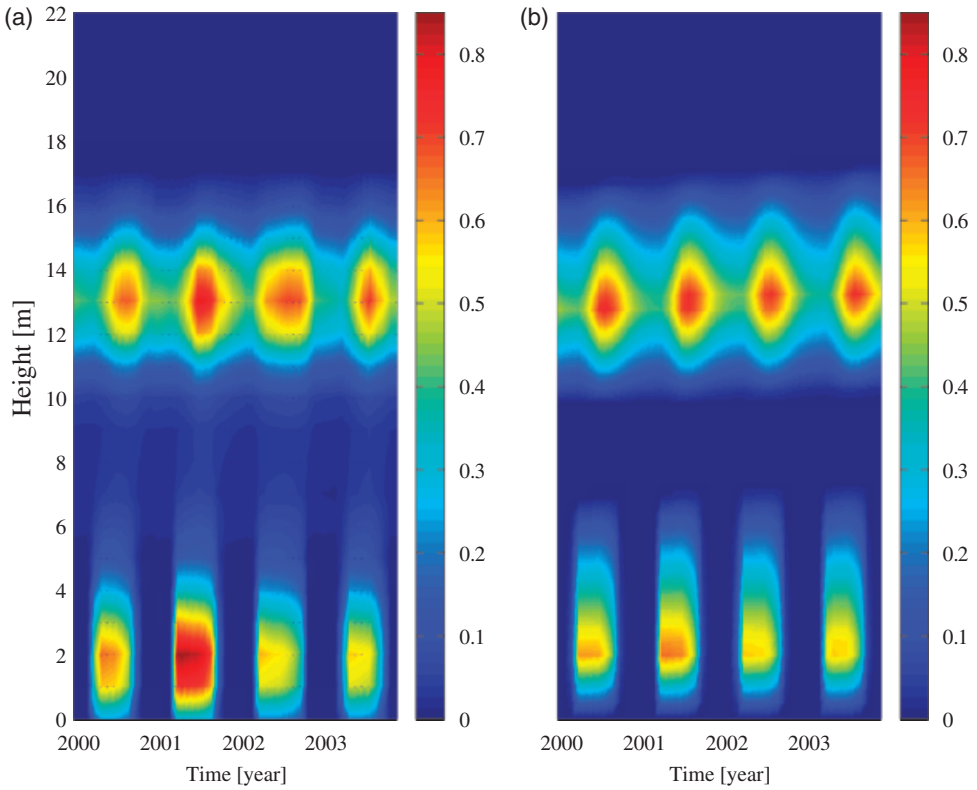

Fig. 2 Time-depth variations (color plots) of leaf area density (*LAD*, $m^2 m^{-3}$) as function of year and height from forest floor. (a) Field estimations of *LAD*. (b) *LAD* modeled by CANVEG with carbon allocation.

values) such as near unity of the regression slope, the small regression intercept, the low root mean square error (RMSE) (about 10% of the highest measured value), and the high correlation coefficient ($r > 0.85$) provides the quantitative support for the apparent good agreement. On the other hand, the model performance for *Fc* and especially *LE* deteriorated during the drought period. The modeled *Fc* was lowered because of constraints on conductance predicted by the Leuning model (Leuning, 1995) following a larger than average *D* experienced during the summer drought period of 2002 (see Fig. 3b). However, this reduction was less than the reduction in the measured *Fc* and degraded statistics, especially the slope and RMSE, and indicates model bias during drought (see Table 2, second set of values). The model overestimated *LE* during the drought (see Fig. 3c). The large driving force experienced in the summer of 2002 more than compensated for the reduction in leaf conductance induced by *D*. This suggests that plant–soil hydraulic system, not included in the model, plays a major role in controlling biosphere–atmosphere gas exchange at this site and only models that account for it can be expected to perform well under limiting moisture conditions.

Model comparison of fluxes – spectral analysis

The Fourier analysis revealed distinct divergence in the correspondence between modeled and measured *NEE* and *ET* (represented by the power spectra of scalar fluxes, Figs 4a and b) across the time scales examined. The scalar flux time series variances (areas under the power spectra) indicate that CANVEG-A captured the spectral energy of both net carbon and water fluxes at intermediate scales, but not at hourly or interannual time scales. Some mechanisms, known to produce significant hourly variability on EC measurements, are not resolved by CANVEG-A. During the day, hourly flux variability is dominated by shifts in footprint size and direction (Oren *et al.*, to appear). At night, passage of clouds and intermittent turbulence are important contributors to the variance at this time scale (Cava *et al.*, 2004). These mechanisms are more related to the intermittent and dynamic nature of the EC measurements (footprint and nighttime storage flushing) and less to physiological processes relevant to forest carbon transfer and storage. The fact that the CANVEG-A model resolved *NEE* at the daily time scales suggests that the effects of dynamic EC footprint and storage

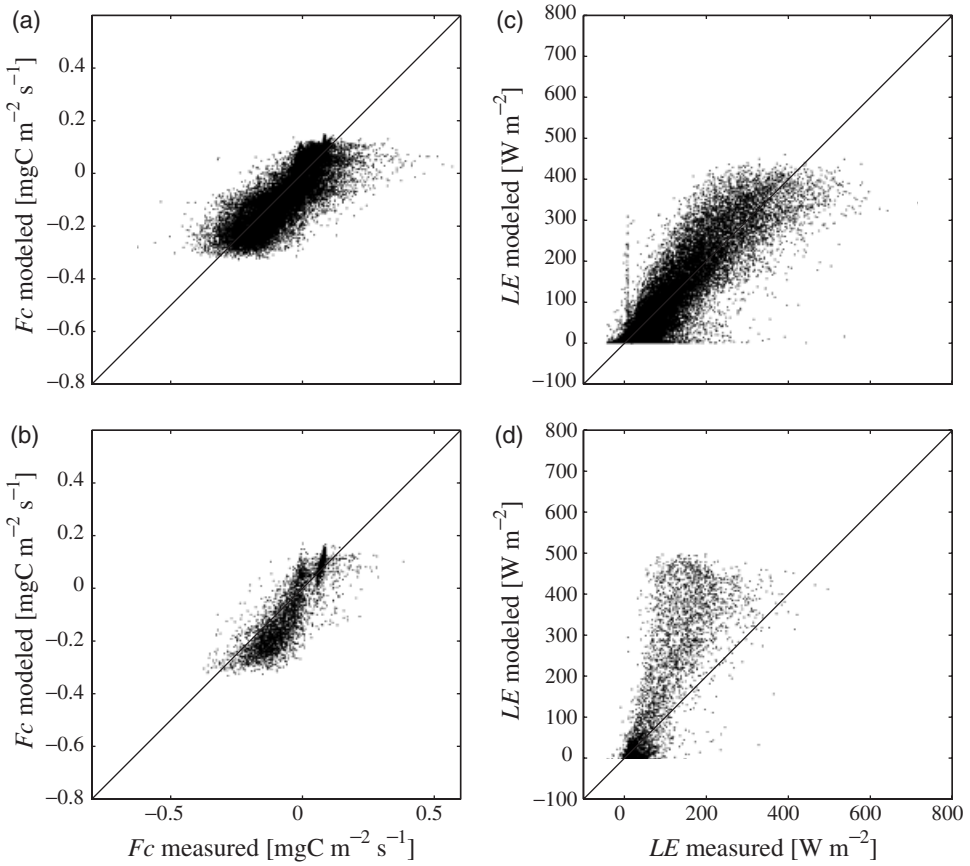

Fig. 3 Comparison of half-hourly CO_2 flux (*Fc*) and latent heat flux (*LE*) measured by the eddy-covariance system and modeled by the CANVEG with carbon allocation (CANVEG-A). Panels (a) and (c) show no water stress runs in the 4-year period and panels (b) and (d) show runs during the drought period (April–September 2002). The 1 : 1 line is shown for reference.

Table 2 Statistics of the regression analysis for measured (abscissa) and 'CANVEG-A' modeled (ordinate) *Fc* (mgC $m^{-2} s^{-1}$), *LE* (W m^{-2}), and *LE* plus sensible heat flux (*LE* + *H* [W m^{-2}]) for runs with no water stress (no ws)

Scalar flux	*Fc*		*LE*		*LE* + *H*	
	no ws	Drought	no ws	Drought	no ws	Drought
Slope*	0.92	1.21	0.99	1.79	0.96	1.07
Intercept†	−0.0074	−0.0077	−0.3	13.9	−4.23	8.61
RMSE†	0.047	0.064	35.2	120.6	50.36	56.48
*r**	0.88	0.90	0.92	0.84	0.94	0.96

The second set of numbers refers to the same statistics but for drought period. RMSE stands for the root mean square error and *r* is the correlation coefficient.
*Indicates a dimensionless statistic.
†Indicates a statistic with the same units as the fluxes.

flushing average out over a day. This is consistent with other studies that specifically focused on footprint averaging (Oren *et al.*, to appear) and storage dynamics (Lai *et al.*, 2000).

At time scales ranging from days to months, CANVEG-A and SECRETS-3PG were able to reproduce the observed variance in *NEE* whereas Biome-BGC underestimated this variability greatly (Fig. 4). The good performance of SECRETS-3PG and the CANVEG-A, and the underestimation by Biome-BGC is related to the ability of the former models to resolve the vertical structure of *LAD* and the inability of the latter model to do so. This point will be explored further in the *LAI* comparisons.

CANVEG-A is the only model that reproduced the variability in *NEE* at seasonal time scales in addition to the daily time scales. Note that the daily and seasonal scales are spectrally the most 'energetic' in this record. All other models underestimated the intraannual variability in *NEE*, and only PnET II was able to capture the seasonal variability in *ET*, although, as we show later, this may be explained by an artifact related to *LAI* dynamics. Thus, CANVEG-A, and to lesser extent SECRETS-3PG, were able to reproduce much of the flux variability at scales shorter than annual. The reason both models performed well at these time scales are

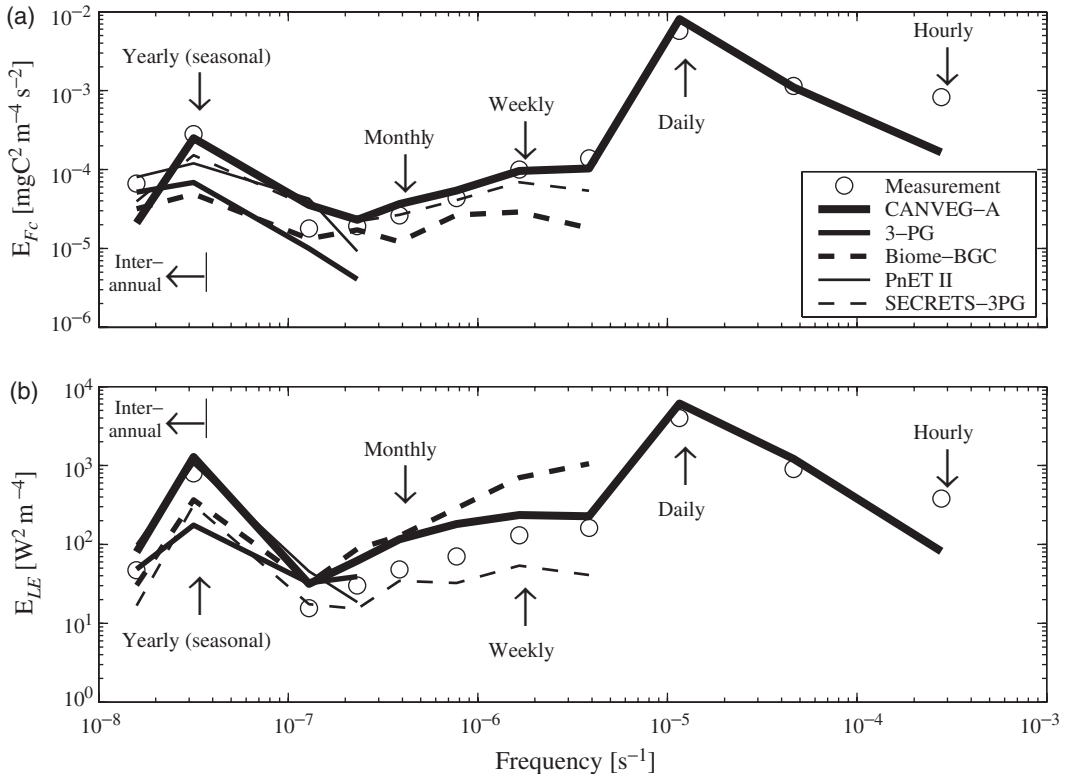

Fig. 4 Measured and modeled power spectra for the CO_2 flux *Fc* [panel (a)] and latent heat flux *LE* [panel (b)].

obvious – they resolve all nonlinearities in their response functions (e.g. photosynthetic response to light) at the leaf scale and correctly integrate this response vertically to the canopy scale. Hence, changes in leaf area density for each species and its nonlinear effect on light attenuation and photosynthesis were explicitly resolved.

Surprisingly, beyond annual time scales, the spectral performance of these models were inconsistent or 'mixed,' as has been found for the mean flux values in another model comparison study (Hanson *et al*., 2004). Although the CANVEG-A (and also Biome-BGC) underestimated interannual variability, PnET II, 3-PG and SECRETS-3PG showed reasonable agreement with the measured value. However, this integration is performed on intraannual variability that was consistently underestimated for both *LE* and *NEE* in all models except for CANVEG-A. This spectral inconsistency or 'mixed' results suggests that good performance of some models on interannual time, scales may be attributed to error cancellations. For *LE*, the contributors to observed pattern in variability may be attributed to *LAI* dynamics, the effects of drought, and averaging of the forcing variables. For *NEE*, additional contributors include estimates of carbon input (*GPP*), and the partitioning of carbon to *NPP*. The mixed spectral performance can originate from several sources that are discussed below.

LAI dynamics

We consider first leaf area dynamics, the primary internal control for carbon input to the system. Time series of modeled monthly values of *LAI* were compared with *LAI* reconstructed from ground measurements (H. McCarthy, personal communication). The understory is a major contributor to total *LAI* variability (Figs 5a and b) because of its contribution to a sharp rise and decay associated with leaf unfolding and senescence. CANVEG-A is the only model designed to estimate *LAI* of a bilayered canopy where the two layers can represent different physiological properties. The model reproduced well the magnitude and dynamics of both the total and pine *LAI* (Fig. 5). This agreement demonstrates that the new allocation scheme captured the dynamics of leaf production and senescence well.

Because 3-PG, Biome-BGC, and PnET II are single-species models and because SECRETS-3PG predicts the *LAI* of the prevailing species, we assess the time series of pine *LAI* in Fig. 5b. PnET II captured well the dynamics of the pine *LAI* rise but predicted unrealistically abrupt decay and it overestimated the peak. Con-

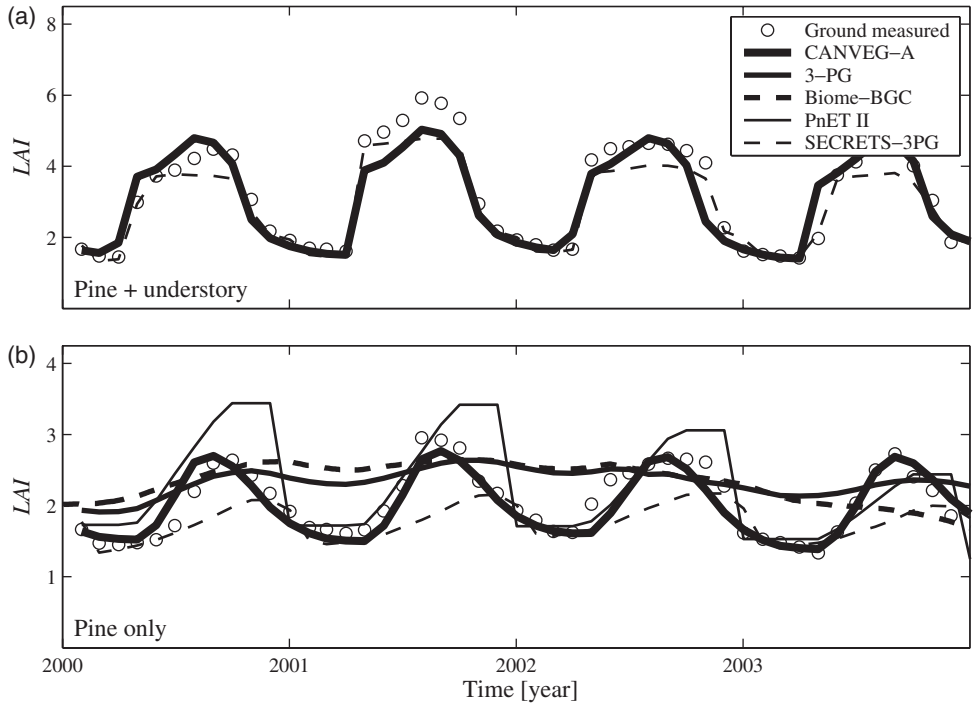

Fig. 5 Comparison between ground-based measured and modeled monthly time series of leaf area index (*LAI*). Panel (a) shows total *LAI* (pine and understory) and panel (b) Pine only *LAI*. Notice the different scale of the panels.

versely, SECRETS-3PG captured the decay in pine *LAI* well but generated too slow a rise to the peak, and the model consistently underestimated the maximum. Biome-BGC and 3-PG exhibited damped variations in *LAI* mostly matching the peaks. An immediate consequence of the '*LAI* dampening' by Biome-BGC and 3-PG is that climatic variability becomes the dominant source of variability in the modeled fluxes at interannual time scales. This seems not to degrade model performance at interannual time scales because the effects of interannual variability in climatic drivers greatly exceed the effects of interannual variability in *LAI* on *LE*. Conversely, PnET II amplifies the seasonal dynamics in *LAI*. This extra variability of *LAI*, added to the variability in climate drivers, increased the variability in *LE* modeled with PnET II when compared with the data (Fig. 4b). For CANVEG-A, the extra interannual variability in *LE* was generated by the absence of control on stomatal conductance by soil moisture availability. This results in unrealistically large *LE* modeled during drought years (25% more than nondrought years; Fig. 3c), because *D* during the drought period was higher then in normal years.

Annual carbon input and allocation analysis

Next, we compare modeled total annual carbon input with the ecosystem to values estimated from EC measurements. Net photosynthesis was estimated from *LE* using

$$GPP \approx g_{\text{canopy}}\, C_a \quad 1 - \frac{\hat{C}_i}{C_a}\Big), \tag{13}$$

where, g_{canopy} is the bulk canopy conductance determined from

$$g_{\text{canopy}} = c' \frac{LE}{1.6\, D} \tag{14}$$

with C_a being the atmospheric CO_2 concentration and $\hat{C}_i$ is the vertically averaged canopy-scale intercellular CO_2 concentration, and c' is a unit conversion.

Two issues complicate the estimation of g_{canopy} from Eqn (14): the first is that *LE* measures both transpiration and evaporation rates; and the second is that when *D* and *LE* are sufficiently small, g_{canopy} remains highly uncertain (Ewers *et al*., 1999). We computed g_{canopy} from 30 min runs for which $PAR > 100\,\mu\text{mol}\,\text{m}^{-2}\,\text{s}^{-1}$ and $D > 0.5$ kPa. Simulations immediately following a rain event were excluded (primarily because instruments were wet) using the precipitation time series, thereby minimizing the contribution of evaporation to *LE*. The limit for above-canopy $PAR > 100\,\mu\text{mol}\,\text{m}^{-2}\,\text{s}^{-1}$ was chosen to ensure that at least a portion of the leaves experienced positive net photosynthesis. The $D > 0.5$ kPa threshold was determined from the mode of the *D* histogram (Fig. 6b, inset). This threshold

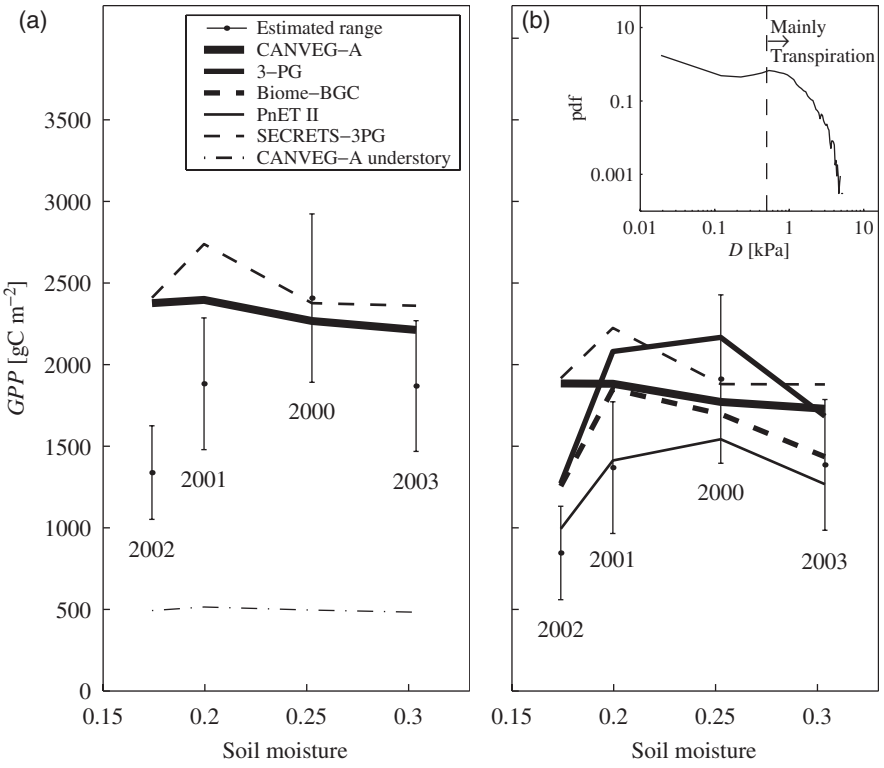

Fig. 6 Comparison between estimated gross primary production (*GPP*) and modeled *GPP*. The inset shows the pdf of vapor pressure deficit (*D*) on a log scale. The upper and lower *GPP* limits (vertical line) were computed assuming $\hat{C}_i/C_a$ is represented by sunlit or shaded foliage, where $\hat{C}_i/C_a$ is the vertically integrated ratio of intercellular to atmospheric CO_2 concentration. Panel (a) represents total *GPP* (pine + understory) and panel (b) represents pine *GPP* only. The estimated range of pine only *GPP* was calculated by subtracting CANVEG with carbon allocation modeled understory *GPP* from the total estimated *GPP*.

maximizes the number of 30-min runs for which the driving force for transpiration is sufficiently large and ensures that the numerical estimation of the conductance remains accurate (Ewers *et al.*, 1999).

We also used stable isotope measurements (Schäfer *et al.*, 2003) for sunlit ($\hat{C}_i/C_a = 0.66$) and shaded ($\hat{C}_i/C_a = 0.78$) foliage to compute 'bounds' on the *GPP* (Fig. 6a). These bounds serve as values that reflect the two *GPP* end members determined by the vertical variability in $\hat{C}_i/C_a$ within the canopy.

The method described above is not able to discern contributions from under- and overstory. To provide some reference to the relative contribution to *GPP* of these two layers, understory *GPP* modeled with CANVEG-A is also shown in Fig. 6a. Because 3-PG, Biome-BGC and PnET II are single-species models, and because the understory *GPP* is a small relative to canopy *GPP* (Fig. 6a), we isolated the contribution of the pines to *GPP* by subtracting the understory *GPP* modeled with CANVEG-A from the total *GPP* (in Fig. 6b). Numerical values of *GPP* are given in Table 3, which also includes *GPP* per unit of *LAI*.

From this analysis we found that:

(1) All models estimated *GPP* within bounds when soil moisture was not limiting, except SECRETS-3PG, which slightly overestimated.
(2) When average soil moisture was less than $0.2\,m^3\,m^{-3}$, CANVEG-A and SECRETS-3PG, both of which do not account for the effects water stress, estimated values above the upper bound of *GPP*.
(3) Of the three single-species models (3-PG, Biome-BGC, and PnET II) that are capable of accounting for soil moisture limitation, pine *GPP* modeled with the original 3-PG and BIOME-BGC followed the observed pattern in *GPP* in relation to soil moisture, with a slight overestimation under water-stress conditions; PnET II predicted values within bounds.

The effect of the drought in 2002 on interannual variation in *GPP* is clearly large (Fig. 6), and models that explicitly considered the drought captured some of the interannual variation. Despite this, the interannual *GPP* variability alone is not sufficient to explain differences of Biome-BGC and PnET II in capturing the spectral energy of *NEE* at the interannual time scale (Fig. 4a). This is not surprising because the power spectrum of

Table 3 Modeled and estimated gross primary production (*GPP*) and net primary production (*NPP*) ($g C m^{-2}$)

Year	Measurement-derived estimates	CANVEG-A	3-PG	PnET II	Biome-BGC	SECRETS-3PG
GPP						
2000	1892–2923					
	(641–991)	2267 (740)	2167 (981)	1543 (627)	1696 (733)	2374 (866)
2001	1479–2286					
	(411–635)	2396 (757)	2080 (841)	1412 (580)	1849 (716)	2738 (852)
2002	1051–1624					
	(316–488)	2376 (766)	1271 (525)	993 (433)	1255 (506)	2409 (801)
2003	1468–2269					
	(508–785)	2212 (738)	1683 (750)	1267 (675)	1435 (723)	2361 (883)
NPP						
2000	833	837 (668)	932	847	579	1170 (796)
2001	756	907 (739)	894	721	684	1356(856)
2002	489	765 (630)	546	351	210	1145(690)
2003	659	729 (584)	724	774	572	1126(697)

The ranges of estimated gross primary production (*GPP*) were calculated using the methodology described in the 'Results.' Values in parentheses are *GPP* per unit of leaf area index (*LAI*) for each model. Estimated net primary productivity (*NPP*) values are calculated from biometry measurements for each year. Values in parentheses are for pine over-story *NPP* only.
Acronyms are described in the text.

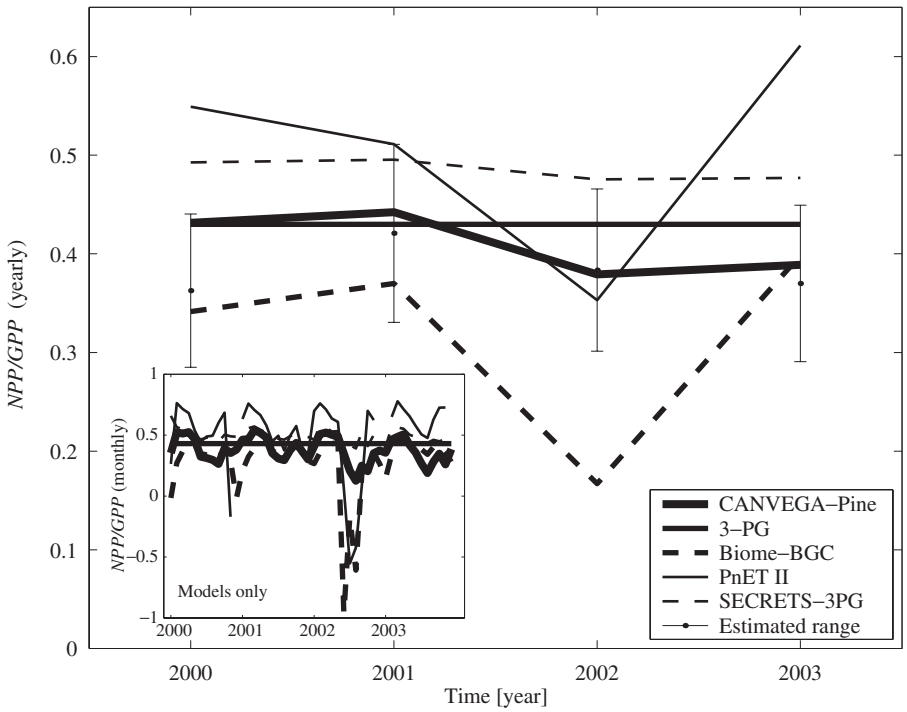

Fig. 7 Modeled net primary production (*NPP*) to gross-primary production (*GPP*) ratio. Note that physiological principles in predicting growth (3-PG) has a constant ratio shown as a straight line. The inset presents the monthly comparisons.

NEE is influenced also by the variability in the partitioning of *GPP* between *NPP* and autotrophic respiration.

At the monthly time scale, the ratio of *NPP* to *GPP* was highly variable and poorly constrained by some models, even reaching negative values during drought (Biome-BGC and PnET II; Fig. 7 inset). The estimated bounds of *NPP*/*GPP* from the annual data show insensitivity to soil moisture variability. At annual time steps, Biome-BCG showed consistent partitioning in years without drought whereas PnET II varied greatly from

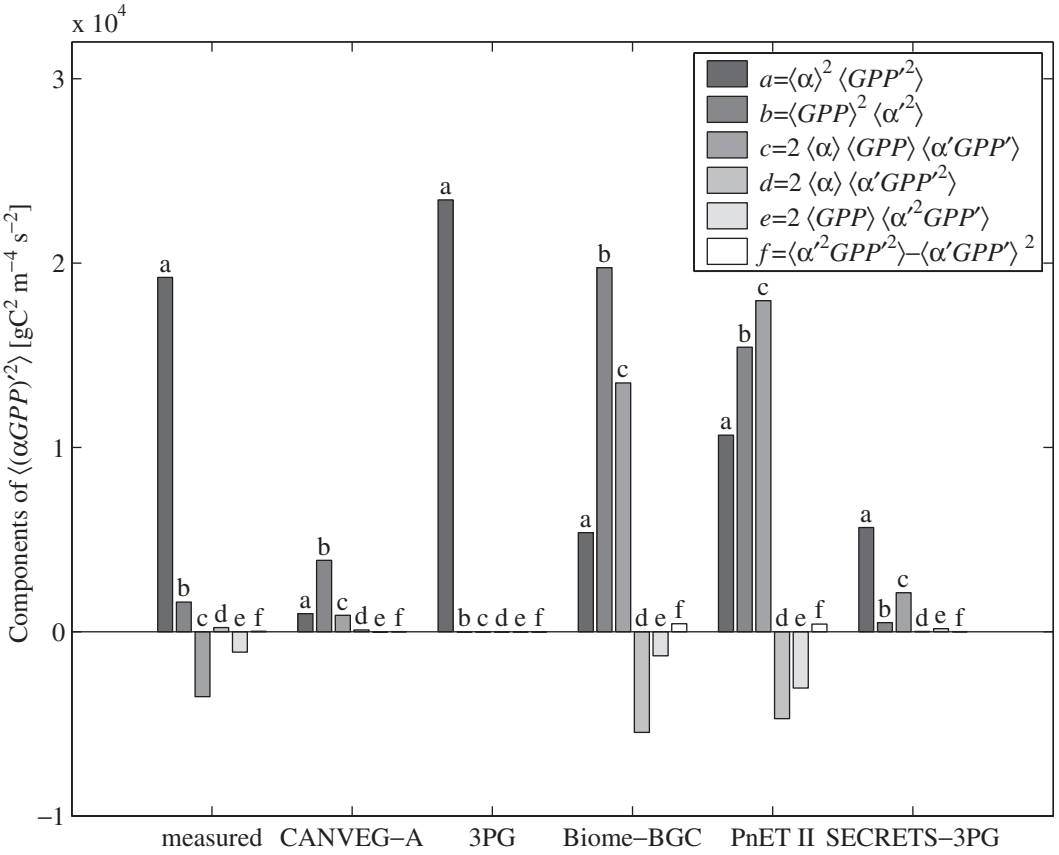

Fig. 8 Components of the expansion of $\langle(\alpha GPP)'^2\rangle$ for measurements and for each model.

year to year even in the absence of a drought. The remaining models predicted nearly invariant *NPP*/*GPP*. During droughts, SECRETS-3PG and PnET II estimated *NPP*/*GPP* that was higher than the upper bound; whereas Biome-BGC estimated a ratio lower than the lower bound.

Variance component analysis

We assessed the relative contribution of variability in *NPP*/*GPP* vs. variability in *GPP*, which is primarily induced by drought, to the interannual variability in *NEE*. Note that

$$NEE = \alpha GPP - R_H, \tag{15}$$

where $\alpha = NPP/GPP$, and R_H is the heterotrophic respiration. It follows that the interannual variability in *NEE* is given by

$$\langle NEE'^2\rangle = \langle(\alpha GPP)'^2\rangle + \langle(R_H')^2\rangle + 2\langle(\alpha GPP)'(R_H')\rangle, \tag{16}$$

where $\langle\cdot\rangle$ is the averaging operator over interannual time scales, and primed quantities denote annual fluctuations from the interannual mean. To explain the spectral inconsistencies in the interannual variability of *NEE* (Fig. 4a) it is necessary to explore how the various models reproduce each term of the *NEE* variance budget (Eqn (16)). Noting that R_H is about 25% of *GPP* (Lai *et al*., 2002; Schäfer *et al*., 2003), and that R_H measurements are not available, we are limited in our assessment to the contribution of $\langle(\alpha GPP)'^2\rangle$ to $\langle NEE'^2\rangle$. The fact that the models must reproduce the proper contribution of $\langle(\alpha GPP)'^2\rangle$ to $\langle NEE'^2\rangle$ is a necessary but not sufficient condition to explain the spectral inconsistencies. We begin by investigating how the various models reproduce the relative contributions of α and *GPP* variability to $\langle(\alpha GPP)'^2\rangle$. In order to do so, we expand $\langle(\alpha GPP)'^2\rangle$ in its components such that the interaction terms are explicit and can be evaluated individually. Some models (e.g. 3-PG) assume that α is constant and

$$\langle(\alpha GPP)'^2\rangle = \langle\alpha\rangle^2\langle GPP'^2\rangle \tag{17}$$

Thus, in 3-PG a reduction in *GPP* results in a proportional reduction in autotrophic respiration ($=(1-\alpha)$ *GPP*).

When both α and *GPP* vary from year to year, the expansion of $\langle(\alpha GPP)'^2\rangle$ is given by the following

six terms:

$$\begin{aligned}
&\langle(\alpha GPP)'^2\rangle = a + b + c + d + e + f,\\
&a = \langle\alpha\rangle^2\langle GPP'^2\rangle,\\
&b = \langle GPP\rangle^2\langle\alpha'^2\rangle,\\
&c = 2\langle\alpha\rangle\langle GPP\rangle\langle\alpha' GPP'\rangle,\\
&d = 2\langle\alpha\rangle\langle\alpha' GPP'^2\rangle,\\
&e = 2\langle GPP\rangle\langle\alpha'^2 GPP'\rangle,\\
&f = \langle\alpha'^2 GPP'^2\rangle - \langle\alpha' GPP'\rangle^2.
\end{aligned} \tag{18}$$

Note that if α is a constant from year to year, then Eqn (18) reduces to the first term (i.e. term *a*). For each model, we compared how the various terms contribute to $\langle(\alpha GPP)'^2\rangle$ (Fig. 8). For measurement-based estimates (Fig. 8) we assumed that the partitioning of sunlit and shaded $\hat{C}_i/C_a$ is 30% and 70%, respectively (Schäfer *et al*., 2003). The assumption of a constant $\hat{C}_i/C_a$ with such weights is justified because across years conductance varies by about a factor of 2 whereas $\hat{C}_i/C_a$ varies by less than 12% (Mortazavi *et al*., 2005). With a constant $\hat{C}_i/C_a$ based on the assumption above, it is possible to evaluate all six components of $\langle(\alpha GPP)'^2\rangle$ for *GPP* modeled from *LE* and *D* data, and using measured *NPP* to evaluate α. The data suggest that the main contributor of $\langle(\alpha GPP)'^2\rangle$ is $\langle\alpha\rangle^2\langle(GPP)'^2\rangle$, in agreement with the 3-PG assumptions in which autotrophic respiration is proportionally related to *GPP*. The CANVEG-A clearly underestimates $\langle\alpha\rangle^2\langle(GPP)'^2\rangle$ because it did not consider the drought effects (Fig. 7). Interestingly, PnET II and Biome-BGC suggest that the variability in *NPP*/*GPP* contributes more to $\langle(\alpha GPP)'^2\rangle$ than the variability in *GPP*, which is inconsistent with the data (Fig. 8). Furthermore, both models predicted that a main contributor to $\langle(\alpha GPP)'^2\rangle$ is a positive $\langle(\alpha GPP')\rangle$ (term c), while the data suggest a negative $\langle(\alpha' GPP')\rangle$. SECRETS-3PG correctly attributed that the variability in $\langle(\alpha GPP)'^2\rangle$ is primarily driven by $\langle\alpha\rangle^2\langle(GPP)'^2\rangle$, but because the drought effects are not considered, the $\langle GPP'^2\rangle$ is highly damped.

Although R_H variability can be important in Eqn (16), we have no explicit data of this quantity. Furthermore, the outcome of the analysis presented in Eqn (18) appears to largely explain the spectral inconsistency in *NEE* (Fig. 8). Earlier we showed that models that account for the reduction in *GPP* because of drought and proportionately reduced autotrophic respiration best explain the interannual variability in *NEE*. Although the results suggest that PnET II also captured the interannual variability of *NEE* (Fig. 4a), this latter analysis shows that the main mechanisms responsible for this variability are not correctly reproduced by PnET II or Biome-BGC. CANVEG-A and SECRETS-3PG underestimated the variability in *NEE* because of the lack of *GPP* response to drought.

Hence, it is safe to say that for this stand, the often-criticized constant *NPP*/*GPP* assumption may be reasonable at interannual time scales because of the constraints this ratio imposes on autotrophic respiration. Furthermore, this ratio may constrain the variability in *NEE* even in future climates experiencing elevated atmospheric CO_2 conditions. Preliminary measurements of *GPP* and *NPP* at the FACE facility within the same stand suggest that elevated atmospheric CO_2 (Schäfer *et al*., 2003) did not alter *NPP*/*GPP*.

Summary and conclusions

The nesting framework used would likely reproduce the entire spectrum of flux variability if realistic plant hydrodynamics can be included. Porous media models for the autotrophic system combined with measured vulnerability curves are a logical first step (Chuang *et al*., 2006). Progress on this issue means that processes at time scales relevant to interstorm periods and soil moisture redistribution must be adequately resolved. It is conceivable that rapid wetting is accompanied by other complex processes such as rapid increase in CO_2 production because of enhanced microbial activity (and hence a concomitant increase in forest floor respiration); however, preliminary investigations suggest that this effect may be small on annual time scales for stands such as in our case study (Palmroth *et al*., 2005). Coupling precipitation, *ET*, and gas-phase CO_2 transfer in the soil to water redistribution following storms using variants on Richards's equation is computationally demanding, and may pose problems that are difficult to overcome. Currently this approach is being implemented and will be subject of future research.

Acknowledgements

This research was supported by the Office of Science (BER), US Department of Energy, through the Terrestrial Carbon Processes Program (TCP) Grant no. DE-FG02-00ER63015 and Grant no DE-FG02-95ER62083, and through BER's Southeast Regional Center (SERC) of the National Institute for Global Environmental Change (NIGEC) under Cooperative Agreement no. DEFC02-03ER63613, by the US Forest Service through the Southern Global Climate Change Program and the Southern Research Station, and by the National Science Foundation's Earth Science Division (NSF-EAR 02-08258).

References

Aber JD, Federer CA (1992) A generalized, lumped-parameter model of photosynthesis, evapotranspiration and net primary production in temperate and boreal forest ecosystems. *Oecologia*, **92**, 463–474.

Aber JD, Ollinger SV, Federer CA *et al*. (1995) Predicting the effects of climate change on water yield and forest production in the northeastern united states. *Climate Research*, **5**, 207–222.

Baldocchi D (1992) A lagrangian random-walk model for simulating water-vapor, CO_2 and sensible heat-flux densities and scalar profiles over and within a soybean canopy. *Boundary-Layer Meteorology*, **61**, 113–144.

Baldocchi D, Falge E, Gu LH *et al*. (2001) Fluxnet: a new tool to study the temporal and spatial variability of ecosystem-scale carbon dioxide, water vapor, and energy flux densities. *Bulletin of the American Meteorological Society*, **82**, 2415–2434.

Baldocchi D, Finnigan J, Wilson K *et al*. (2000) On measuring net ecosystem carbon exchange over tall vegetation on complex terrain. *Boundary-Layer Meteorology*, **96**, 257–291.

Baldocchi D, Meyers T (1998) On using eco-physiological, micrometeorological and biogeochemical theory to evaluate carbon dioxide, water vapor and trace gas fluxes over vegetation: a perspective. *Agricultural and Forest Meteorology*, **90**, 1–25.

Butnor JR, Johnsen KH, Oren R *et al*. (2003) Reduction of forest floor respiration by fertilization on both carbon dioxide-enriched and reference 17-year-old loblolly pine stands. *Global Change Biology*, **9**, 849–861.

Campbell GS, Norman JM (1998) *An Introduction to Environmental Biophysics*. Springer-Verlag New York Inc, New York, NY, USA.

Cava D, Giostra U, Siqueira M *et al*. (2004) Organised motion and radiative perturbations in the nocturnal canopy sublayer above an even-aged pine forest. *Boundary-Layer Meteorology*, **112**, 129–157.

Chuang TL, Bertozzi AL, Oren R (2006) Modeling transpiration rates from sap flow data using the porous media analogy. *Ecological Modelling*, **19**, 447–468.

Collatz GJ, Ball JT, Grivet C *et al*. (1991) Physiological and environmental-regulation of stomatal conductance, photosynthesis and transpiration – a model that includes a laminar boundary-layer. *Agricultural and Forest Meteorology*, **54**, 107–136.

dePury DGG, Farquhar GD (1997) Simple scaling of photosynthesis from leaves to canopies without the errors of big-leaf models. *Plant Cell and Environment*, **20**, 537–557.

Ellsworth DS (2000) Seasonal CO_2 assimilation and stomatal limitations in a Pinus Taeda canopy. *Tree Physiology*, **20**, 435–445.

Ellsworth DS, Oren R, Huang C *et al*. (1995) Leaf and canopy responses to elevated CO_2 in a pine forest under free-air CO_2 enrichment. *Oecologia*, **104**, 139–146.

Ewers BE, Oren R, Albaugh TJ *et al*. (1999) Carry-over effects of water and nutrient supply on water use of Pinus Taeda. *Ecological Applications*, **9**, 513–525.

Field GD, Mooney HA (1996) The photosysthesis–nitrogen relationship in wild plants. In: *On the Economy of Plant Form and Function* (ed. Givinish TJ), Cambridge University Press, New York, 22–55.

Hacke UG, Sperry JS, Ewers BE *et al*. (2000) Influence of soil porosity on water use in Pinus Taeda, **124**, 495–505.

Hamilton JG, DeLucia EH, George K *et al*. (2002) Forest carbon balance under elevated CO_2. *Oecologia*, **131**, 250–260.

Hamilton JG, Thomas RB, Delucia EH (2001) Direct and indirect effects of elevated CO_2 on leaf respiration in a forest ecosystem. *Plant Cell and Environment*, **24**, 975–982.

Hanson PJ, Amthor JS, Wullschleger SD *et al*. (2004) Oak forest carbon and water simulations: model intercomparisons and evaluations against independent data. *Ecological Monographs*, **74**, 443–489.

Hsieh CI, Katul G, Chi T (2000) An approximate analytical model for footprint estimation of scalar fluxes in thermally stratified atmospheric flows. *Advances in Water Resources*, **23**, 765–772.

IPCC (2001) IPCC Third Assessment Report. Intergovernmental Panel in Climate Change.

Jarvis PG (1995) Scaling processes and problems. *Plant Cell And Environment*, **18**, 1079–1089.

Kaimal JC, Finnigan JJ (1994) *Atmopheric Boundary Layer Flows: Their Structure and Measurements*. Oxford Press, Oxford.

Katul GG, Albertson JD (1999) Modeling CO_2 sources, sinks, and fluxes within a forest canopy, **104**, 6081–6091.

Katul GG, Chang WH (1999) Principal length scales in second-order closure models for canopy turbulence, **38**, 1631–1643.

Katul GG, Ellsworth DS, Lai CT (2000) Modelling assimilation and intercellular CO_2 from measured conductance: a synthesis of approaches. *Plant Cell and Environment*, **23**, 1313–1328.

Katul G, Hsieh CI, Kuhn G *et al*. (1997) Turbulent eddy motion at the forest–atmosphere interface. *Journal of Geophysical Research – Atmospheres*, **102**, 13409–13421.

Katul G, Lai CT, Schäfer K *et al*. (2001) Multiscale analysis of vegetation surface fluxes: from seconds to years, **24**, 1119–1132.

Kimball JS, Thornton PE, White MA *et al*. (1997a) Simulating forest productivity and surface-atmosphere carbon exchange in the BOREAS study region. *Tree Physiology*, **17**, 589–599.

Kimball JS, White MA, Running SW (1997b) Biome-BGC simulations of stand hydrologic processes for BOREAS. *Journal of Geophysical Research – Atmospheres*, **102**, 29043–29051.

Lai CT, Katul G, Butnor J *et al*. (2002) Modelling night-time ecosystem respiration by a constrained source optimization method. *Global Change Biology*, **8**, 124–141.

Lai CT, Katul G, Ellsworth D *et al*. (2000) Modelling vegetation-atmosphere CO_2 exchange by a coupled Eulerian–Langrangian approach. *Boundary-Layer Meteorology*, **95**, 91–122.

Landsberg JJ, Johnsen KH, Albaugh TJ (2001) Applying 3-PG, a simple process-based model designed to produce practical results, to data from loblolly pine experiments, **47**, 43–51.

Landsberg JJ, Waring RH (1997) A generalised model of forest productivity using simplified concepts of radiation-use efficiency, carbon balance and partitioning. *Forest Ecology and Management*, **95**, 209–228.

Leuning R (1995) A critical-appraisal of a combined stomatal-photosynthesis model for C-3 plants. *Plant Cell and Environment*, **18**, 339–355.

McMurtrie RE, Landsberg JJ (1992) Using a simulation-model to evaluate the effects of water and nutrients on the growth and carbon partitioning of Pinus Radiata. *Forest Ecology and Management*, **52**, 243–260.

Medlyn BE, Dewar RC (1999) Comment on the article by R. H. Waring, J. J. Landsberg and M. Williams relating net primary production to gross primary production. *Tree Physiology*, **19**, 137–138.

Meiresonne L, Sampson DA, Kowalski AS *et al*. (2003) Water flux estimates from a belgian scots pine stand: a comparison of different approaches. *Journal of Hydrology*, **270**, 230–252.

Mortazavi B, Chanton JP, Prater JL *et al*. (2005) Temporal variability in C-13 of respired CO_2 in a pine and a hardwood forest subject to similar climatic conditions. *Oecologia*, **142**, 57–69.

Naidu SL, DeLucia EH, Thomas RB (1998) Contrasting patterns of biomass allocation in dominant and suppressed loblolly pine. *Canadian Journal of Forest Research – Revue Canadienne De Recherche Forestiere*, **28**, 1116–1124.

Naumburg E, Ellsworth DS, Katul GG (2001) Modeling dynamic understory photosynthesis of contrasting species in ambient and elevated carbon dioxide. *Oecologia*, **126**, 487–499.

Oren R, Ewers BE, Todd P *et al*. (1998) Water balance delineates the soil layer in which moisture affects canopy conductance. *Ecological Applications*, **8**, 990–1002.

Oren R, Hsieh CI, Stoy P *et al*. (to appear) Estimating the uncertainty in annual net ecosystem carbon exchange originating from spatial variability in turbulent fluxes and sampling errors in eddy-covariance measurements. *Global Change Biology*.

Oren R, Sperry JS, Katul GG *et al*. (1999) Survey and synthesis of intra- and interspecific variation in stomatal sensitivity to vapour pressure deficit. *Plant Cell and Environment*, **22**, 1515–1526.

Palmroth S, Maier CA, McCarthy HR *et al*. (2005) Contrasting responses to drought of forest floor CO_2 efflux in a loblolly pine plantation and a nearby oak-hickory forest. *Global Change Biology*, **11**, 421–434.

Running SW, Coughlan JC (1988) A general-model of forest ecosystem processes for regional applications.1. Hydrologic balance, canopy gas-exchange and primary production processes. *Ecological Modelling*, **42**, 125–154.

Ryan MG, Hubbard RM, Pongracic S *et al*. (1996) Foliage, fine-root, woody-tissue and stand respiration in Pinus Radiata in relation to nitrogen status. *Tree Physiology*, **16**, 333–343.

Sampson DA, Albaugh TJ, Johnsen KH *et al*. (2003) Monthly leaf area index estimates from point-in-time measurements and needle phenology for Pinus Taeda. *Canadian Journal of Forest Research – Revue Canadienne De Recherche Forestiere*, **33**, 2477–2490.

Sampson DA, Ceulemans R (1999) Secrets: simulated carbon fluxes from a mixed coniferous/deciduous Belgian forest. In: *Forest Ecosystem Modelling, Upscaling and Remote Sensing* (eds Ceulemans R, Veroustraete F, Gond V, VanRensbergen J), SPB Academic Publishing, The Hague, 99–108.

Sampson DA, Janssens IA, Ceulemans R (2001) Simulated soil CO_2 efflux and net ecosystem exchange in a 70-year-old Belgian scots pine stand using the process model secrets. *Annals of Forest Science*, **58**, 31–46.

Sampson DA, Waring RH, Maier CA *et al*. (2006) Fertilization effects on forest carbon storage and exchange and net primary production; a new hybrid process model for stand management. *Forest Ecology and Management*, **221**, 91–109.

Schäfer KVR, Oren R, Ellsworth DS *et al*. (2003) Exposure to an enriched CO_2 atmosphere alters carbon assimilation and allocation in a pine forest ecosystem. *Global Change Biology*, **9**, 1378–1400.

Siqueira M, Katul G (2002) Estimating heat sources and fluxes in thermally stratified canopy flows using higher-order closure models. *Boundary-Layer Meteorology*, **103**, 125–142.

Sit V, Poulin-Costello M (1994) *Catalog of Curve for Curve Fitting, Ministry of Forest Research Program, Biometric Infromation Handbook No. 4*. Crown Publications, Victoria, BC, Canada.

Stenberg P (1998) Implications of shoot structure on the rate of photosynthesis at different levels in a coniferous canopy using a model incorporating grouping and penumbra. *Functional Ecology*, **12**, 82–91.

Stoy PC, Katul GG, Siqueira MB *et al*. (2005) Variability in net ecosystem exchange from hourly to inter-annual time scales at adjacent pine and hardwood forests: a wavelet analysis. *Tree Physiology*, **25**, 887–902.

Stull RB (1988) *An Introduction to Boundary Layer Meteorology*. Kluwer Academic Publishers, Dordrecht.

Thornley JM (1998) *Grasslands Dynamics: An Ecosystem Simulation Model*. CAB International, Wallingford, UK.

Thornton PE, Law BE, Gholz HL *et al*. (2002) Modeling and measuring the effects of disturbance history and climate on carbon and water budgets in evergreen needleleaf forests. *Agricultural And Forest Meteorology*, **113**, 185–222.

Waring RH, Landsberg JJ, Williams M (1998) Net primary production of forests: a constant fraction of gross primary production? *Tree Physiology*, **18**, 129–134.

Webb EK, Pearman GI, Leuning R (1980) Correction of flux measurements for density effects due to heat and water-vapor transfer. *Quarterly Journal of the Royal Meteorological Society*, **106**, 85–100.